

# Comparative study of screened inter-layer interactions in the Coulomb drag effect in bilayer electron systems

R. Asgari,<sup>1</sup> B. Tanatar,<sup>2</sup> and B. Davoudi<sup>3</sup>

<sup>1</sup>*Institute for Studies in Theoretical Physics and Mathematics, Tehran 19395-5531, Iran*

<sup>2</sup>*Department of Physics, Bilkent University, Bilkent, 06800 Ankara, Turkey*

<sup>3</sup>*Département de Physique and Centre de Recherche en Physique du Solide, Université de Sherbrooke, Sherbrooke, Québec, Canada J1K 2R1*

Coulomb drag experiments in which the inter-layer resistivity is measured are important as they provide information on the Coulomb interactions in bilayer systems. When the layer densities are low correlation effects become significant to account for the quantitative description of experimental results. We investigate systematically various models of effective inter-layer interactions in a bilayer system and compare our results with recent experiments. In the low density regime, the correlation effects are included via the intra- and inter-layer local-field corrections. We employ several theoretical approaches to construct static local-field corrections. Our comparative study demonstrates the importance of including the correlation effects accurately in the calculation of drag resistivity. Recent experiments performed at low layer densities are adequately described by effective inter-layer interactions incorporating static correlations.

PACS numbers: 73.40.-c, 73.21.Ac, 73.40.Kp

## I. INTRODUCTION

In the last decade transport properties of dilute two-dimensional (2D) electron and hole systems have amassed a great interest. Much of the excitement and controversy is centered around the temperature dependence of resistivity which appears to exhibit metallic behavior at high densities and insulating behavior at low densities.<sup>1</sup> In bilayer systems in which the barrier separating the coupled quantum wells is large enough so that tunneling effects are negligible, the inter-layer resistivity has been measured for more than a decade.<sup>2</sup> In this so-called drag effect the momentum transfer between the layers is measured.<sup>3</sup> In contrast to the single layer resistivity which shows a nontrivial interplay between interaction and disorder effects near the metal-insulator transition<sup>4</sup>, the inter-layer resistivity is largely determined by the long range Coulomb scattering (as long as the single layer densities are away from metal-insulator transition region). Therefore Coulomb drag experiments provide valuable information on the intra- and inter-layer electron-electron interactions especially when the layer densities are lowered.

Over the years there has been a number of Coulomb drag experiments at zero magnetic field using different samples and probing different parameter regimes. The main parameters entering a drag experiment set-up are the layer density  $n$  which may be related to the dimensionless coupling strength  $r_s$  (for the definition of  $r_s$  see Section II), the separation distance between the layers  $d$  and the Fermi temperature  $T_F$ . Hill *et al.*<sup>5</sup> measured drag resistivity  $\rho_D$  in an electron bilayer system at densities corresponding to  $1.13 \lesssim r_s \lesssim 1.57$  and high temperatures  $T \sim T_F$ . The observed peak in  $\rho_D$  around  $T \approx T_F/2$  was attributed to the contribution of plasmons. In fact, the experimental results were regarded

as an indirect evidence for the existence of acoustic and optical plasmons in a bilayer system.<sup>6</sup> Similar experiments were also performed by Noh *et al.*<sup>7</sup> confirming plasmon effects on the drag resistivity and revealing the importance of possible dynamic correlations even though the layer densities were such that  $r_s \approx 1.48$  where the strong coupling effects are not expected. More recent experiments by Kellogg *et al.*<sup>8</sup> used samples with layer densities reaching  $r_s \approx 4.3$  and  $k_F d \sim 1$  where  $d$  is the center-to-center well separation. In contrast to the above experiments, Pillarisetty *et al.*<sup>9</sup> measured frictional drag between two dilute 2D hole layers in which the  $r_s$  values were in the range  $19 \leq r_s \leq 39$ .

On the theoretical side, the drag resistivity has first been formulated within the random-phase approximation (RPA) for the layer density-response functions and inter-layer effective interaction.<sup>10,11</sup> Here and most subsequent works treat the inter-layer effective interaction as given by the bare inter-layer Coulomb interaction screened by the bilayer system dielectric function. Importance of dynamical correlations is noticed even at the RPA level since the difference between the static and dynamic screening function brings quantitative changes to the drag resistivity.<sup>10</sup> At larger  $r_s$  values when the correlation effects become significant one should go beyond the RPA. One way to do this in a physically motivated way is through the local-field corrections to the RPA form of the screening function. The simplest form of the local-field corrections is the Hubbard approximation which was used by Hill *et al.*<sup>5</sup> to analyze their data. A much widely used local-field corrections are calculated within the self-consistent field approximation scheme of Singwi *et al.*<sup>12</sup> (STLS). They have been incorporated in the evaluation of the drag resistivity by Świerkowski *et al.*<sup>13</sup>. In connection with the Kellogg *et al.* experiments<sup>8</sup>, Yurtsever *et al.*<sup>14</sup> pointed out that STLS local-field corrections yield a poor representation and suggested the use of a different effective interaction originally developed by Kukkonen and Overhauser<sup>15</sup> and Vignale and Singwi.<sup>16</sup> Recently, Badalyan *et al.*<sup>17</sup> employed frequency dependent local-field corrections in the long-wavelength limit ( $q \rightarrow 0$ ) obtained from dynamical exchange-correlation kernel in the context of density functional theory.

In this work we investigate systematically the effect of the form of screened inter-layer interaction on the temperature dependence of drag resistivity. We calculate the drag resistivity employing several models for the inter-layer interaction and compare their behavior with the experimental results of Kellogg *et al.*<sup>8</sup> which provide a useful test at low density. As input to various theoretical models of inter-layer interaction we consider several constructs of local-field corrections. Our calculations reveal the importance of the choice of inter-layer interaction model and the significant role played by the local-field corrections.

The rest of this paper is organized as follows. In Sec. II, we introduce the models for inter-layer interaction that enters the drag resistivity. We then outline the calculation of local-field corrections in various approaches. Section III contains our numerical calculations of drag resistivity and comparison of models with experimental data. We conclude

in Sec. IV with a brief summary.

## II. THEORETICAL APPROACH

We consider a double-quantum-well structure with  $d$  as the center-to-center well separation such that there is no tunneling between them and  $L$  as the width of the quantum wells. Each layer is characterized by the dimensionless coupling constant  $r_s a_B^* = 1/\sqrt{\pi n}$  where  $n$  is the areal density,  $a_B^* = \hbar^2 \epsilon / (m^* e^2)$  is the effective Bohr radius,  $\epsilon$  and  $m^*$  being the background dielectric constant and electron band effective mass. Each layer has only one type of charge carrier, i.e. electrons, although our theoretical formulation could be applicable to hole-hole and electron-hole layers with suitable changes. In the case of electron-hole bilayers the prospect of formation of an excitonic state<sup>18</sup> and its detection through drag experiments<sup>19</sup> requires a new formulation of the effective inter-layer interaction which we do not address here. However, correlations in electron-hole bilayers and their effects on drag resistivity can be studied using the improved inter-layer models we shall describe below. The motion of the carriers is free along the  $xy$  plane and under the action of a double-well potential profile in the  $z$ -direction only the lowest subband in each quantum well is occupied. For this aim, temperature should be less than the difference between excited energy level and the ground state energy in quantum well. This yields  $T < 3(r_s a_B^*/L)^2 T_F/16$ . Furthermore, the bilayer system is assumed to be embedded in a uniform neutralizing positive background charge. The unscreened Coulomb interaction potential, in Fourier space, between the electrons in  $k$ th and  $l$ th layers is given by  $v_{kl}(q) = v_q F_{kl}(qL)$ . Here,  $v_q = 2\pi e^2/(\epsilon q)$  and  $F_{kl}$  are infinite quantum-well form factors taking the finite width effects into account which are given by<sup>10</sup>

$$\begin{aligned} F_{kk}(x) &= \frac{3x + 8\pi^2/x}{x^2 + 4\pi^2} - \frac{32\pi^4[1 - \exp(-x)]}{x^2(x^2 + 4\pi^2)^2} \\ F_{kl}(x) &= \frac{64\pi^4 \sinh^2(x/2)}{x^2(x^2 + 4\pi^2)^2} \exp(-qd). \end{aligned} \quad (1)$$

We note that most theoretical calculations<sup>6,10,13</sup> adopt the infinite quantum-well model to account for the width effects, whereas a better way would be to calculate the Coulomb matrix elements using envelope functions  $\phi_n(z)$  determined self-consistently from the Poisson and Schrödinger equations.<sup>20</sup>

The drag resistivity (or as it is also called transresistivity)  $\rho_D$  of an electron system at temperature  $T$  has been obtained in a variety of theoretical models. These include diagrammatic perturbation theory<sup>10,21</sup>, the Boltzmann equation<sup>22</sup> and the memory function formalism<sup>11,13</sup>. In a drag experiment one applies an electric field  $E_1$  to layer 1 (drive layer) creating a current to flow with current density  $J_1$ . This sets up an electric field  $E_2$  in layer 2 (drag layer) where no current is allowed to flow. The drag resistivity is defined as  $\rho_D = E_2/J_1$  and the microscopic calculations relate this quantity to the rate of change of momentum between the layers, as electron-electron inter-layer interactions

transfer momentum from the drive layer with carrier density  $n_1$  to the drag layer with density  $n_2$ .

Theoretical considerations lead to the same expression for  $\rho_D$  in terms of the effective inter-layer interaction and the density-response function of the single layers. When the effective inter-layer interaction treated perturbatively,  $\rho_D$  is given as

$$\rho_D = -\frac{\hbar^2}{8\pi^2 e^2 n_1 n_2 k_B T} \int_0^\infty q^3 dq \int_0^\infty d\omega \frac{|W_{12}(q, \omega)|^2 \Im m \chi_1^0(q, \omega, T) \Im m \chi_2^0(q, \omega, T)}{\sinh^2(\hbar\omega/2k_B T)}, \quad (2)$$

where  $\chi_i^0(q, \omega)$ , ( $i = 1$  or  $2$ ) is the non-interacting linear response corresponding to the drive and drag layer which shows the charge density fluctuations in a given layer at finite temperature and  $W_{12}(q, \omega)$  is the effective inter-layer interaction.

An important ingredient which is needed to calculate  $\rho_D$  is the electron-electron inter-layer interaction,  $W_{12}(q, \omega)$ . The effective electron-electron interaction for a two-component system given by a  $2 \times 2$  matrices and in random-phase approximation (RPA) it is given by

$$\hat{W}_{RPA}(q, \omega) = \hat{v}(q) + \hat{v}(q) \hat{\chi}(q, \omega) \hat{v}(q), \quad (3)$$

where  $\hat{\chi}(q, \omega)$  defined in terms of the non-interacting charge-charge response function and Coulomb interactions.

To take into account the effect of correlations more clearly, which are more important in the strongly correlated regime where  $r_s$  becomes large, we need more sophisticated approaches. For this purpose, we introduce here other approximation scheme for  $W_{12}(q, \omega)$  proposed by Świerkowski *et al.*<sup>13,17</sup> (SSG) where

$$\hat{W}_{SSG}(q, \omega) = v_{eff}^i(q) + \hat{v}_{eff}(q) \hat{\chi}(q, \omega) \hat{v}_{eff}(q), \quad (4)$$

where  $v_{eff}^{ij}(q) = v_{ij}(q)(1 - G_{ij}(q))$  are the effective Coulomb interactions and  $G_{ij}(q)$  are intra- and inter local-field corrections (LFC) which take into account multiple scattering to infinite order between all components of the plasma compared with the RPA where these effects are neglected.

A more detailed analysis, which accounts for the vertex corrections associated with charge-charge fluctuation, was carried out for an electron gas (EG) in Refs. 14,16,23, where Kukkonen-Overhauser-like effective inter-layer interaction potential<sup>15</sup> were obtained by different approaches. In this scheme we have

$$\hat{W}_{VS}(q, \omega) = \hat{v}_{eff}(q) + \hat{v}_{eff}(q) \hat{\chi}(q, \omega) \hat{v}_{eff}(q) - \hat{U}, \quad (5)$$

with the elements of  $\hat{U}$  defined by  $v_{ij}(q)G_{ij}(q)$ . The form of  $W_{12}(q, \omega)$  within the Vignale and Singwi (VS) approach is similar to that in the self-consistent field approach of Singwi *et al.*<sup>12,13</sup> (SSG) except for the last term. More clearly,

the inter-layer interaction in Eq. (5) is given by<sup>16,23</sup>

$$W_{12}(q, \omega)|_{VS} = \frac{v_{12}(q)(1 - G_{12}(q))}{\Delta(q, \omega)} - v_{12}(q)G_{12}(q), \quad (6)$$

where

$$\Delta(q, \omega) = [1 - v_{11}(q)(1 - G_{11}(q))\chi_1^0(q, \omega, T)](1 - v_{22}(q)(1 - G_{22}(q))\chi_2^0(q, \omega, T)] - [v_{12}(q)(1 - G_{12}(q))]^2 \chi_1^0(q, \omega, T) \chi_2^0(q, \omega, T). \quad (7)$$

Here  $\chi_k^0(q, \omega, T)$  is non-interacting charge-charge response function at finite temperature.<sup>6</sup>

Another approximation scheme for screened bilayer 2D electron-electron interaction is proposed by Zheng and MacDonald<sup>24</sup>(ZM). In this scheme the screened electron-electron interaction potential is given as

$$\hat{W}_{ZM}(q, \omega) = [1 - \hat{\chi}^0(q, \omega, T)\hat{v}_{eff}(q)]^{-1} \hat{v}(q). \quad (8)$$

This is derived essentially from a two-component generalization of the vertex function that enters in self-energy in the so-called  $G\Gamma$  approximation. However, because of the matrix nature of two-component systems there seems to be some ambiguity in such a construction. Note, for instance, that  $\hat{W}_{ZM}$  is not a symmetric matrix for unmatched bilayer systems. Finally, we remark that VS, SSG and ZM forms of the effective electron-electron interactions reduce to RPA if the LFCs are omitted.

As it is clear from Eqs. (4), (5) and (8) the local-field corrections are the fundamental quantities for an evaluation of the effective electron-electron interaction. Here, we intend to examine the inter-layer potential of the Coulomb bilayer system by including correlation effects. To this purpose, we made use of the STLS approach both at zero (STLS0) and finite temperature (STLS) schemes. The STLS theory embodies correlations beyond the RPA approach and as an important improvement. In this approach the static LFC that accounts for correlation effects among carriers in the layers  $k$  and  $l$  are given by:

$$G_{kl}(q) = -\frac{1}{n} \int \frac{d\mathbf{q}'}{(2\pi)^2} \frac{\mathbf{q} \cdot \mathbf{k}}{q^2} \frac{v_{kl}(q')}{v_{kl}(q)} [S_{kl}(|\mathbf{q} - \mathbf{q}'|) - \delta_{kl}], \quad (9)$$

where  $S_{kl}(q)$  is a static structure factor. The equations of motion for the Wigner distribution functions in a bilayer coupled with the linear-response theory yield in the Singwi *et al*<sup>12</sup> approach the following expression for the density-density response functions:

$$\chi_{kl}(q, \omega) = \frac{\chi_k^0(q, \omega, T) \{ \delta_{kl} + (-1)^{\delta_{kl}} v_{kl}(q)(1 - G_{kl}(q))\chi_l^0(q, \omega, T) \}}{\Delta(q, \omega)}. \quad (10)$$

The fluctuation-dissipation theorem leads to the static structure factor for a bilayer at finite temperature

$$S_{kl}(q) = -\frac{\hbar}{\pi \sqrt{n_k n_l}} \int d\omega \Im m \chi_{kl}(q, \omega) \coth \left( \frac{\hbar\omega}{2k_B T} \right). \quad (11)$$

Equations (9), (10) and (11) are solved numerically in a self-consistent way for  $G_{kl}(q)$  both at zero and finite temperature cases separately.

Another sophisticated method is based on Fermi hypernetted-chain approach (FHNC). Our strategy follows a similar approach to our recent works, Ref. [25] which uses accurate intra- and inter-layer static structure factors to build the local-field corrections. For this purpose we implement the self consistent Fermi hypernetted-chain approach<sup>26,27,28</sup> at zero temperature in order to calculate the intra- and inter-layer static structure factors incorporating the finite thickness effects in a quantum well. The latter effects are known to be important for the adequate description of the drag resistivity from a number of calculations.<sup>6,10,13,17</sup> In what follows we explain the FHNC approximation and then outline our method to obtain the static local-field corrections,  $G_{ij}(q)$ , at zero temperature.

With the zero of energy taken at the chemical potential, the formally exact differential equation for the pair-correlation function<sup>29</sup>,  $g_{\alpha\beta}(r)$ , and following Chakraborty<sup>30</sup> using the two-component plasma Jastrow-Slater variational theory involving FHNC approximation, reads

$$\left[ -\frac{\hbar^2}{m}\nabla^2 + V_{\alpha\beta}^{eff}(r) \right] \sqrt{g_{\alpha\beta}(r)} = 0 \quad , \quad (12)$$

where  $m$  is electron mass and  $V_{\alpha\beta}^{eff}(r) = v_{\alpha\beta}(r) + W_{\alpha\beta}^B(r) + W_{\alpha\beta}^F(r)$ . In Eq. (12) we decompose the effective potential into three terms  $v_{\alpha\beta}(r)$ ,  $W_{\alpha\beta}^B$  and  $W_{\alpha\beta}^F$  of which the last two terms take into account correlation and exchange effects respectively, we substitute to the direct boson potential  $W_{\alpha\beta}^B$  the one calculated by Chakraborty<sup>30</sup> for a two component Bose system using the static structure factors  $S_{\alpha\beta}(k)$  of a Fermi system:

$$\begin{cases} W_{\alpha\alpha}^B(k) = -\frac{\hbar^2 k^2}{4mn_\alpha} [2S_{\alpha\alpha}(k) - 3 + (S_{\alpha\bar{\alpha}}^2(k) + S_{\alpha\bar{\alpha}}^2(k))/\Gamma^2(k)] \\ W_{\alpha\bar{\alpha}}^B(k) = -\frac{\hbar^2 k^2}{4m\sqrt{n_\alpha n_{\bar{\alpha}}}} [2S_{\alpha\bar{\alpha}}(k) - S_{\alpha\bar{\alpha}}(k)(S_{\alpha\bar{\alpha}}(k) + S_{\alpha\alpha}(k))/\Gamma^2(k)] \end{cases} \quad (13)$$

Here  $S_{\alpha\beta}(k) = \delta_{\alpha\beta} + \sqrt{n_\alpha n_\beta} \int [g_{\alpha\beta}(r) - 1] \exp(i\mathbf{k} \cdot \mathbf{r}) d\mathbf{r}$  is the static structure factor and

$$\Gamma(k) = S_{11}(k)S_{22}(k) - S_{12}^2(k) . \quad (14)$$

Turning to the exchange term  $W_{\alpha\beta}^F$ , it is itself defined in order to make Eq. (12) exact and has a very complicated expression within the FHNC.<sup>26,27,28</sup> However, in dealing with a one-component electron fluid, Kallio and Piilo<sup>31</sup> have proposed a simple and efficient way to account for the antisymmetry of the fermion wave function. Their argument is immediately generalized to our two-component Fermi fluid, and leads to the requirement that, in the high density regime in both layers, the Hartree-Fock pair distribution functions are solution of Eq. (12). Following this prescription,

it turns out that  $W_{\alpha\beta}^F(k)$  is given by,

$$W_{\alpha\alpha}^F(k) = \int \frac{\hbar^2}{m} \frac{\nabla_{\mathbf{r}}^2 \sqrt{g_{\alpha\alpha}^{\text{HF}}(r)}}{\sqrt{g_{\alpha\alpha}^{\text{HF}}(r)}} e^{i\mathbf{k}\mathbf{r}} d\mathbf{r} + \frac{\hbar^2 k^2}{4mn_{\alpha}} \left[ 2S_{\alpha\alpha}^{\text{HF}}(k) - 3 + \left( \frac{1}{S_{\alpha\alpha}^{\text{HF}}(k)} \right)^2 \right], \quad (15)$$

and  $W_{\alpha\alpha}^F(k) = 0$ . In Eq. (15) we used the fact that the Coulomb term in Eq. (12) becomes negligible in the Hartree-Fock limit with respect to the kinetic term.

Although the expression for the exchange potential in Eq. (15) is correct only for weakly coupled Fermi fluids, we shall assume in the following that it can yield useful results in our self-consistent calculations of the pair distribution functions with increasing coupling strength<sup>29</sup>. As a broad qualitative argument in support of this assumption we may remark that the role of the statistics is expected to weaken with increasing coupling strength making the correlation term dominate on the exchange one. In Eq. (15)  $S_{\alpha\alpha}^{\text{HF}}(k)$  and  $g_{\alpha\alpha}^{\text{HF}}(r)$  are, respectively, the static structure factor and the intra-layer pair distribution functions in the Hartree-Fock approximation (HF), namely

$$S_{\alpha\alpha}^{\text{HF}}(k) = \frac{2}{\pi} \left[ \arcsin \left( \frac{k}{2k_{F_{\alpha}}} \right) + \frac{k}{2k_{F_{\alpha}}} \sqrt{1 - \left( \frac{k}{2k_{F_{\alpha}}} \right)^2} \right] \vartheta(2k_{F_{\alpha}} - k) + \vartheta(k - 2k_{F_{\alpha}}), \quad (16)$$

and  $g_{\alpha\alpha}^{\text{HF}}(r) = 1 - 2(j_1(rk_{F_{\alpha}})/rk_{F_{\alpha}})^2$  and  $g_{\alpha\alpha}^{\text{HF}}(r) = 1$ , where  $j_1$  is a spherical Bessel function, and  $k_{F_{\alpha}} = (2\pi n_{\alpha})^{1/2}$ .

It is evident that the insertion of Eqs. (13-16) into Eq. (12) allows a self-consistent calculation of the pair distribution functions and of the effective interactions. The fluctuation-dissipation theorem which is of paramount importance for systems in equilibrium relates the dynamic susceptibilities defined above to the static structure factors allows one to determine the local-field corrections once the static structure factors are calculated by FHNC approach<sup>25</sup>.

### III. NUMERICAL RESULTS

In this section we present our calculations for drag resistivity  $\rho_D$  using the theoretical models described above and compare them with the recent experimental measurements. We proceed to illustrate our main numerical results, which are summarized in Figs. 1-7.

The effective inter-layer interaction models which go beyond the RPA use local-field corrections as input. In Fig. 1, we display the typical behavior of intra- and inter-layer LFCs  $G_{11}(q)$  and  $G_{12}(q)$ , respectively. We note that whereas the LFCs in the STLS approach have a monotone  $q$  dependence, FHNC approach yields a peaked structure. Such a structure in static LFCs is well known from quantum Monte Carlo simulations<sup>32</sup> and it is thought to represent the correlation effects correctly. Thus, differences in LFCs will evidently play an important role in the drag resistivity. We also remark that there is considerable difference between zero and finite temperature (at  $T = 1$  K) STLS calculations especially for the inter-layer LFC,  $G_{12}(q)$ . We believe that within our calculational scheme the FHNC approach yields

the most accurate LFCs. To illustrate our point, we compare the intra- and inter-layer pair-correlation functions  $g_{\alpha\beta}(r)$  resulting from FHNC calculations and QMC simulations<sup>17</sup> in Fig. 2(a). We note that the agreement is very good. The STLS scheme does not reproduce well the peak structure in  $g_{11}(r)$  at this density which corresponds to  $r_s = 7.07$ . We have also looked at the inter-layer distance  $d$  dependence of the LFCs within the FHNC approach. Figure 2(b) shows intra- and inter-layer LFCs for various values of  $d$  at a layer density  $n = 3.1 \times 10^{10} \text{ cm}^{-2}$ . We have also used the finite quantum-well widths corresponding to Kellogg *et al.*<sup>8</sup> experimental sample. As expected, the intra-layer LFC  $G_{11}(q)$  is not affected much as  $d$  changes, whereas the inter-layer LFC  $G_{12}(q)$  becomes smaller in magnitude as  $d$  increases, reflecting the weakened Coulomb correlations. Similar qualitative results have also been found in a bilayer STLS calculation.<sup>33</sup>

In Figs. 3 and 4 we show the calculated drag resistivity as a function of temperature for various theoretical models of effective inter-layer interaction (i.e. models denoted as VS, SSG and ZM) with different LFCs (i.e. schemes denoted as FHNC, STLS and STLS0) at layer densities  $3.1 \times 10^{10} \text{ cm}^{-2}$  and  $3.8 \times 10^{10} \text{ cm}^{-2}$  and compare them with the experimental results of Kellogg *et al.*<sup>8</sup> The experimental data were obtained for bilayer GaAs-AlGaAs heterostructures for two identical infinite layers of electrons separated by  $d = 280 \text{ \AA}$  and with a double quantum well of widths  $L = 180 \text{ \AA}$ . In all our results, the drag resistivity calculated within the VS inter-layer potential is larger than the one calculated within the SSG approximation. It means that the value of  $U$  increases with increasing  $G_{12}(q)$ , and VS potential in Eq. (5) becomes highly different from the SSG potential given by Eq. (4). The static LFCs which are constructed within the FHNC approach together with the electron-electron inter-layer potential calculated within VS and SSG approaches give results in quite good agreement with experimental measurements especially in the low temperature regime below the plasmon-mediated drag. In these figures, the RPA results underestimate the experimental results. Therefore, after the inclusion of many-body effects correctly (such as using FHNC), the drag resistivity is in good quantitative agreement with experimental results. The LFCs in STLS scheme yield an overestimate of drag resistivity when it is calculated using the VS and SSG inter-layer potentials,  $W_{12}(q, \omega)$ . From the physical point of view, correlation effects suppress the energies of both the acoustic and optical plasmons, while finite temperature effects tend to increase the energies. From this cancellation, the STLS0/SSG gives results close to the experimental data in comparison to STLS/SSG. Furthermore, the value of intra-layer LFC at finite temperature at a given  $q < 2k_F$  value, is smaller than the intra-layer LFC at zero temperature in STLS0 scheme and this yields to have larger plasmon contribution in drag resistivity when one employs the zero temperature LFCs. Furthermore, the inter-layer LFC at zero temperature is larger than the one at finite temperature, thus the drag resistivity in STLS0/Vs is further overestimated than in STLS/Vs approach.

Figure 5 shows the log-log plot of the drag resistivity  $\rho_D$  as a function of layer density at  $T = 1$  and 4 K. For comparison with recent calculations of drag resistivity by Badalyan *et al.*<sup>17</sup>, we extract their results from Fig. 15 (denoted in the figure by BKVS) and compare them with the results of our calculations, mainly FHNC/VS and FHNC/SSG. Evidently, our FHNC calculation produces better agreement with experiment in the whole range of density compared to all other approximations.

The low temperature behavior of drag resistivity  $\rho_D$  for the samples of Kellogg *et al.*<sup>8</sup> is important in understanding the interaction effects. The low density and close inter-layer spacing such that  $k_F d \lesssim 1$  implies significant contributions of backward scattering processes to  $\rho_D$  and predicts deviations from the usual  $T^2$  dependence.<sup>2</sup> These deviations expected to be in the form  $\sim T^2 \ln T$  are difficult to be assessed, but the sensitivity of  $\rho_D$  to layer densities has been noted. In Fig. 6 we show the scaled drag resistivity  $\rho_D/T^2$  as a function of temperature for  $n = 3.8 \times 10^{10} \text{ cm}^{-2}$  and  $n = 2.3 \times 10^{10} \text{ cm}^{-2}$ . The drag resistivity including the FHNC local-field corrections through the various screened inter-layer interaction models is compared with RPA. We note that VS and SSG screened inter-layer interaction models reproduce the upturn behavior of  $\rho_D/T^2$  at low temperature observed in the Kellogg *et al.*<sup>8</sup> experiments. On the other hand, ZM model predicts an opposite behavior in contradiction with experiments. The increase in  $\rho_D/T^2$  at low temperatures due to exchange-correlation effects were first analyzed by Badalyan *et al.*<sup>17</sup> where they used the static local-field corrections in this temperature regime. Similar enhancement in scaled drag resistivity was also obtained by Hwang *et al.*<sup>34</sup> in their calculation on bilayer hole systems in connection with the experiments of Pillarisetty *et al.*<sup>9</sup> Our comparative study thus provides information as to which form of screened inter-layer interaction is more suitable in describing drag experiments at low density.

Finally, we display the inter-layer distance dependence of the many-body correlation effects on drag resistivity in Fig. 7. When the layer separation is decreased, inter-layer Coulomb interaction enhances and this leads to an increase in drag resistivity. Because the Kellogg *et al.*<sup>8</sup> experiment did not measure  $\rho_D$  for samples with different  $d$  values, we are not able to make a systematic comparison.

In the examples above we have seen that the local-field factors play a significant role in the quantitative description of the measured drag resistivity. It is important to remark that the drag resistivity is calculated for electron-electron interaction only and we ignore other scattering processes (i.e. impurities, phonons, etc.) which may be effective in realistic situations. In general, the theoretical prediction by the results of Eq. (2) should yield values below the experimental measurements for drag resistivity in which all scattering process are included.<sup>11,22,35</sup> Since our calculations already provide a very good agreement with Kellogg *et al.*<sup>8</sup> we can argue that phonon and impurity effects are not very important for these samples. The phonon contribution is identified by the peak in  $\rho_D/T^2$  which

occurs when the average thermal phonon wave vector becomes comparable to  $2k_F$ . The Kellogg *et al.*<sup>8</sup> data do not show such a peak. Disorder in general enhances the drag resistivity and in particular when the electron or hole layers are close to metal-insulator transition it plays a very important role.<sup>9</sup> We have not systematically studied the disorder effect here but judging from the results of our comparison to Kellogg *et al.*<sup>8</sup> data we surmise that it is not significant.

We also note that we model the finite width of experimental sample by an infinite square well which modifies the bare potentials by a form factor. The effect of correct form factor and its parameters (barrier height, etc.) obtained by well geometry may be crucial in the final results for drag resistivity. We have not done a self-consistent calculation of a realistic bilayer structure to test this. Variations up to 20% in the quantum-well width  $L$ , however, does not seem to affect the drag resistivity at low temperatures.

#### IV. SUMMARY

We have investigated the performance of various models of inter-layer electron-electron interactions on the temperature dependence of drag resistivity. Such models going beyond the RPA are necessary to account for increasing correlation effects at low density. A major input to construct an effective inter-layer interaction is local-field corrections. We have considered the self-consistent field approach of Singwi *et al.*<sup>12</sup> both at zero and finite temperature and FHNC formalism to obtain intra- and inter-layer local-field corrections. Our calculations compared with relevant experimental results of Kellogg *et al.*<sup>8</sup> demonstrate the importance of including correlation effects correctly in the drag resistivity formula. The effective interaction model developed by Vignale and Singwi<sup>16</sup> supplemented by local-field corrections from FHNC approach provides very good quantitative agreement with experiments. Furthermore, previous application<sup>14</sup> of the VS effective interaction model with simplified local-field corrections find justification in the present calculations. In the temperature range of Kellogg *et al.* experiments<sup>8</sup> where the plasmon contribution should not be significant, static local-field corrections account for the observed drag resistivity.

It would be of interest to develop frequency dependent local-field corrections at a similar level of sophistication presented in this work to investigate the dynamic correlations. They are expected to be important for the plasmon-mediated drag occurring at high temperatures ( $T \sim T_F$ ) as discussed by Flensberg and Hu<sup>6</sup> and most recently by Badalyan *et al.*<sup>17</sup> Especially, single- and multi-pair decay mechanisms when properly incorporated in the dynamic correlations may explain the observed behavior<sup>7</sup> of drag resistivity in bilayers with unmatched densities. Another possible direction is to study the phonon-mediated drag for low density systems which should be effective at layer separations larger than those considered in this work.

## Acknowledgments

We are grateful to G. Vignale for illuminating discussions and comments. We thank B.Y.-K. Hu for discussions at an earlier stage. This work is supported by TUBITAK (106T052) and TUBA.

- 
- <sup>1</sup> For a recent review of the current status of the field see, S. V. Kravchenko and M. P. Sarachik, Rep. Prog. Phys. **67**, 1 (2004).  
<sup>2</sup> T.J. Gramila, J.P. Eisenstein, A.H. MacDonald, L.N. Pfeiffer, and K.W. West, Phys. Rev. Lett. **66**, 1216 (1991); Phys. Rev. B **47**, 12957 (1993); U. Sivan, P.M. Solomon, H. Shtrikman, Phys. Rev. Lett. **68**, 1196 (1992); H. Rubel, E.H. Linfield, D.A. Ritchie, K.M. Brown, M. Pepper, and G.A.C. Jones, Semicond. Sci. Technol. **10**, 1229 (1996).  
<sup>3</sup> For a review see , A. G. Rojo, J. Phys.: Condens. Matter **11**, R31 (1999).  
<sup>4</sup> A. Punnoose and A.M. Finkelstein, Science **310**, 289 (2005).  
<sup>5</sup> N.P.R. Hill, J.T. Nicholls, E.H. Linfield, M. Pepper, D.A. Ritchie, G.A.C. Jones, BenYu-Kuang Hu, and K. Flensberg, Phys. Rev. Lett. **78**, 2204 (1997).  
<sup>6</sup> K. Flensberg and BenYu-Kuang Hu, Phys. Rev. B **52**, 14796 (1995).  
<sup>7</sup> H. Noh, S. Zelakiewicz, X.G. Feng, T.J. Gramila, L.N. Pfeiffer, and K.W. West, Phys. Rev. B **58**, 12621 (1998).  
<sup>8</sup> M. Kellogg, J.P. Eisenstein, L.N. Pfeiffer, and K.W. West, Solid State Commun. **123**, 515 (2002).  
<sup>9</sup> R. Pillarisetty, H. Noh, D.C. Tsui, E.P. De Poortere, E. Tutuc, and M. Shayegan, Phys. Rev. Lett. **89**, 016805 (2002).  
<sup>10</sup> A.P. Jauho and H. Smith, Phys. Rev. B **47**, 4420 (1993).  
<sup>11</sup> L. Zheng and A.H. MacDonald, Phys. Rev. B **48**, 8203 (1993).  
<sup>12</sup> K.S. Singwi, M.P. Tosi, R.H. Land, and A. Sjölander, Phys. Rev. **176**, 589 (1968).  
<sup>13</sup> L. Świerkowski, J. Szymanski, Z.W. Gortel, Phys. Rev. Lett. **74**, 3245 (1995); Phys. Rev. B **55**, 2280 (1997).  
<sup>14</sup> A. Yurtsever, V. Moldoveanu and B. Tanatar, Solid State Commun. **125**, 575 (2003) .  
<sup>15</sup> C.A. Kukkonen and A.W. Overhauser, Phys. Rev. B **20**, 550 (1979).  
<sup>16</sup> G. Vignale and K.S. Singwi, Phys. Rev. B **31**, 2729 (1985).  
<sup>17</sup> S.M. Badalyan, C.S. Kim, G. Vignale, and G. Senatore, Phys. Rev. B **75**, 125321 (2007) .  
<sup>18</sup> S. De Palo, F. Rapisarda, and G. Senatore, Phys. Rev. Lett. **88**, 206401 (2002) and references therein.  
<sup>19</sup> G. Vignale and A.H. MacDonald, Phys. Rev. Lett. **76**, 2786 (1996); BenYu-Kuang Hu, Phys. Rev. Lett. **85**, 820 (2000).  
<sup>20</sup> D.S. Kainth, D. Richards, H. P. Hughes, M. Y. Simmons, and D. A. Ritchie, J. Phys.: Condens. Matter **12**, 439 (2000).  
<sup>21</sup> A. Kamenev and Y. Oreg, Phys. Rev. B **52**, 7516 (1995).  
<sup>22</sup> K. Flensberg, BenYu-Kuang Hu, A.P. Jauho, and J.M. Kinaret, Phys. Rev. B **52**, 14 761 (1995).  
<sup>23</sup> C.F. Richardson and N.W. Aschroft, Phys. Rev. B **55**, 15130 (1997).  
<sup>24</sup> L. Zheng and A.H. MacDonald, Phys. Rev. B **49**, 5522 (1994) .  
<sup>25</sup> R. Asgari, A.L. Subaşı, A.A. Sabouri-Dodaran, and B. Tanatar, Phys. Rev. B **74**, 155319 (2006); R. Asgari and B. Tanatar, Phys. Rev. B **74** , 075301 (2006); R. Asgari, A. Esmilian, and B. Tanatar, Solid State Commun. **141**, 595 (2007); R. Asgari, Solid State Commun. **141**, 563 (2007) .  
<sup>26</sup> L.J. Lantto and P.J. Siemens, Nuclear Phys. A **317**, 55 (1979); L.J. Lantto, Phys. Rev. B **36**, 5160 (1987) .  
<sup>27</sup> J.G. Zabolitzky, Phys. Rev. B **22**, 2353 (1980) .  
<sup>28</sup> E. Krotscheck and M. Saarela, Phys. Rep. **232**, 1 (1993) .  
<sup>29</sup> S. Abedinpour, R. Asgari, M. Polini, and M. P. Tosi, To appear in Solid State Commun. (2007); B. Davoudi, R. Asgari, M. Polini, and M. P. Tosi, Phys. Rev. **B68** 155112 (2003) .  
<sup>30</sup> T. Chakraborty, Phys. Rev. B **25**, 3177 (1982); **26**, 6131 (1982); T. Chakraborty, A. Kallio, L.J. Lantto, and P. Pietiläinen, Phys. Rev. B **27**, 3061 (1983) .  
<sup>31</sup> A. Kallio and J. Piilo, Phys. Rev. Lett. **77**, 4237 (1996) .  
<sup>32</sup> G. Senatore, S. Moroni, and D. M. Ceperley, in *Quantum Monte Carlo Methods in Physics and Chemistry*, eds. M. P. Nightingale and C.J. Umrigar, (Kluwer, 1999), p. 183; S. Moroni, D. M. Ceperley, and G. Senatore, Phys. Rev. Lett. **69**, 1837-1840 (1992).  
<sup>33</sup> L. Liu, L. Swierkowski, D. Neilson, and J. Szymanski, Phys. Rev. B **53**, 7923 (1996).  
<sup>34</sup> E.H. Hwang, S. Das Sarma, V. Braude, and A. Stern, Phys. Rev. Lett. **90**, 086801 (2003).  
<sup>35</sup> Ben Yu-Kuang Hu, Phys. Rev. B **57**, 12345 (1998); K. Guven and B. Tanatar, Phys. Rev. B **56**, 7535 (1997); B. Tanatar, Phys. Rev. B **58**, 1154 (1998).

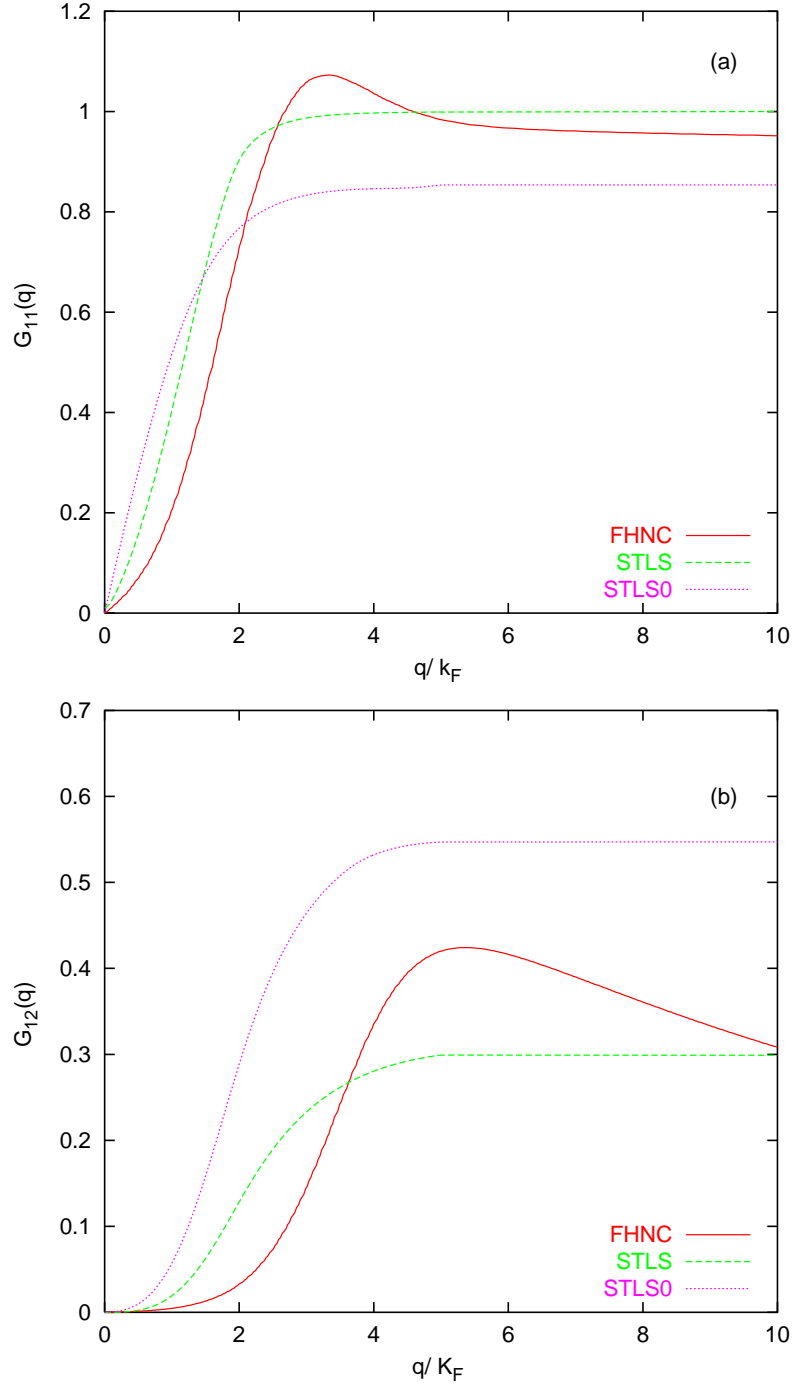


FIG. 1: (Color online) The local-field corrections (LFC) in various models. (a) Intra-layer LFC  $G_{11}(q)$ , (b) inter-layer LFC  $G_{12}(q)$ . Solid, dashed, and dotted lines correspond to FHNC, STLS (at  $T = 1$  K), and STLS0, respectively. The calculations are for equal density layers ( $n = 3.1 \times 10^{10} \text{ cm}^{-2}$ ) and sample parameters are as in Ref. 8.

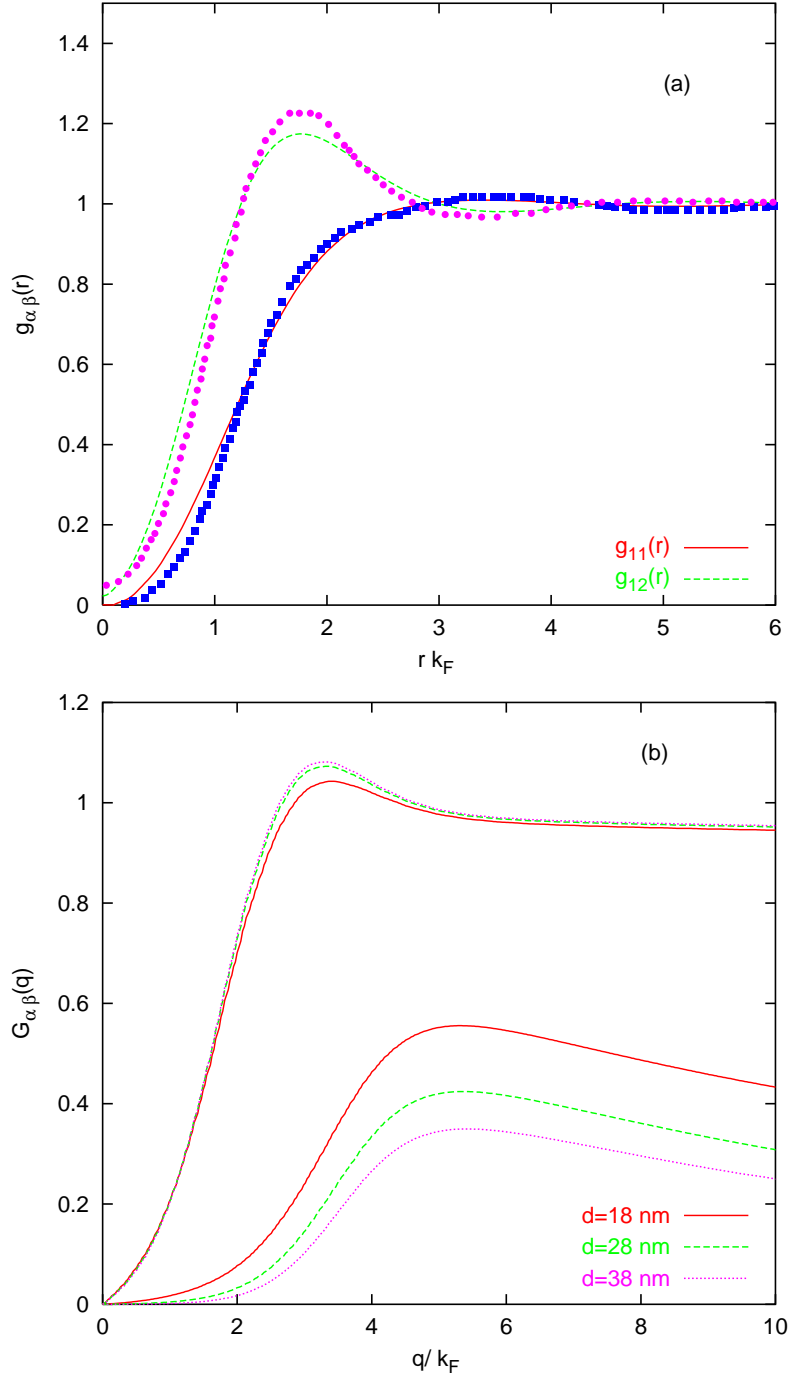


FIG. 2: (Color online) (a) The intra- and inter-layer pair-correlation functions at  $r_s = 7.07$  calculated within the FHNC approach in comparison with QMC results of Ref. 17 (b) The intra- and inter-layer local-field corrections (LFC) at  $n = 3.1 \times 10^{-10} \text{ cm}^{-2}$  ( $r_s = 3.25$ ) calculated within the FHNC approach for different inter-layer distances  $d$ .

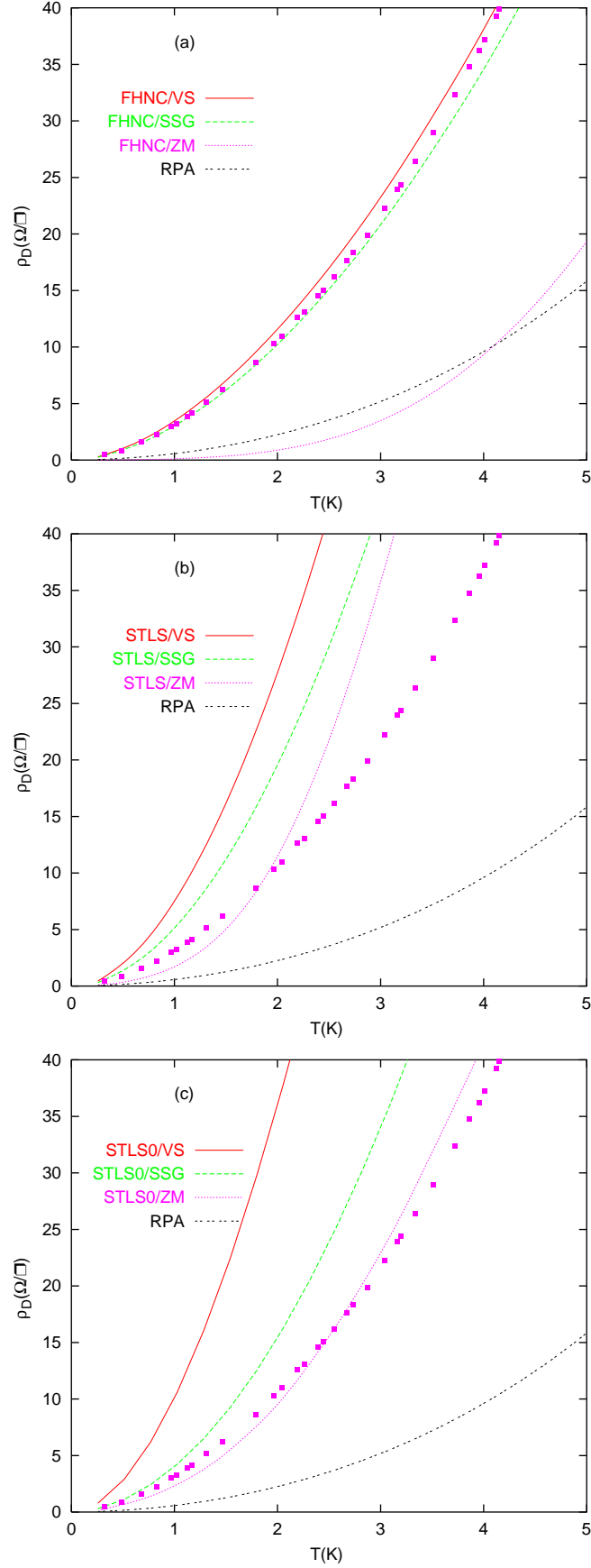


FIG. 3: (Color online) The temperature dependence of the drag resistivity for the identical bilayer electron-electron systems for  $n = 3.1 \times 10^{10} \text{ cm}^{-2}$  ( $r_s = 3.25$ ). The full boxes are the experimental data of Ref. 8. (a) FHNC, (b) STLS, and (c) STLS0 local-field corrections are used in conjunction with different screened inter-layer interaction models.

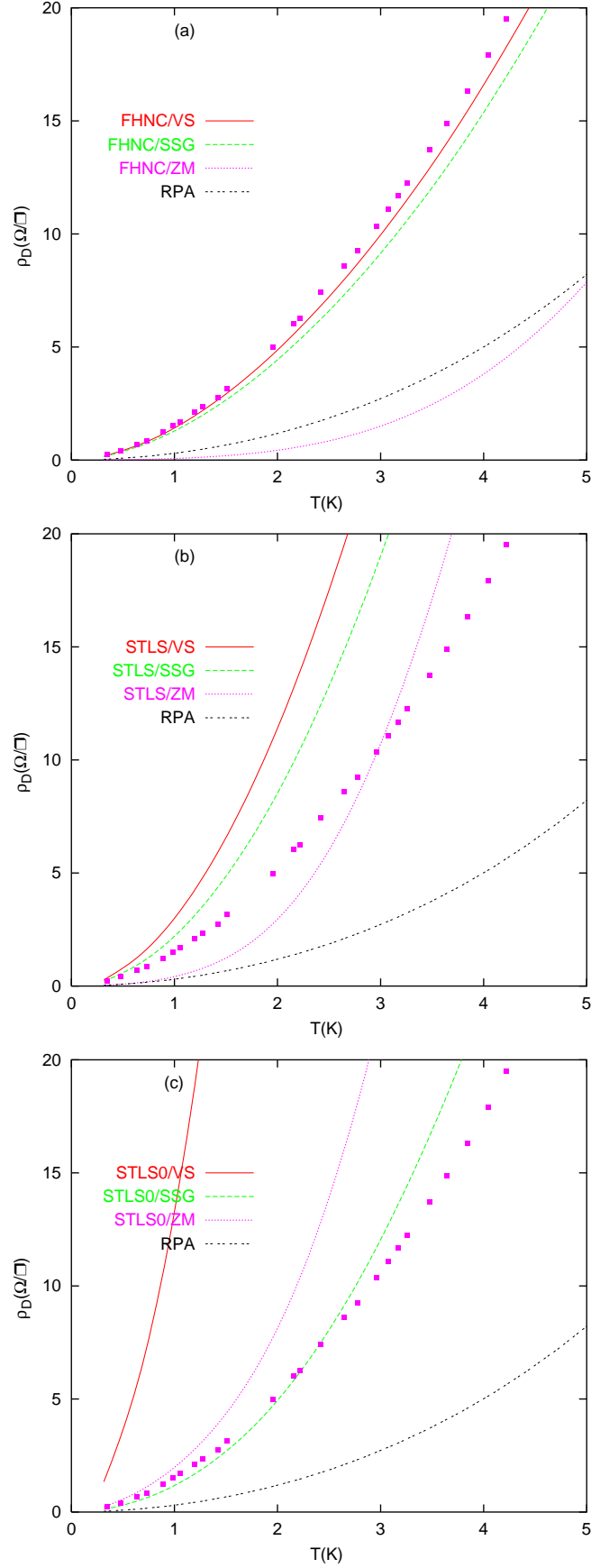


FIG. 4: (Color online) The temperature dependence of the drag resistivity for the identical bilayer electron-electron systems for  $n = 3.8 \times 10^{10} \text{ cm}^{-2}$  ( $r_s = 2.93$ ). The full boxes are the experimental data of Ref. 8. (a) FHNC, (b) STLS, and (c) STLS0 local-field corrections are used in conjunction with different screened inter-layer interaction models.

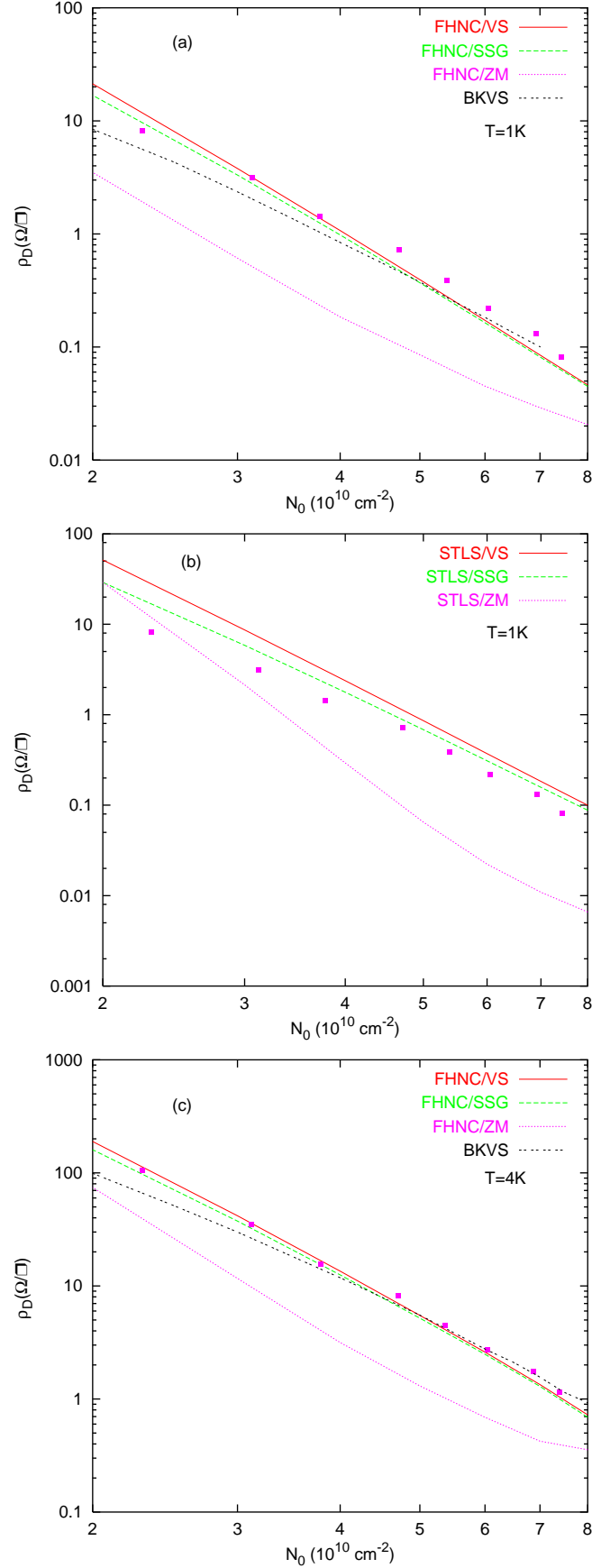


FIG. 5: (Color online) The density dependence of the drag resistivity for the identical bilayer electron-electron systems at  $T = 1$  and  $4\text{ K}$  in a log-log plot. The full boxes are the experimental data of Ref. 8. BKVS refers to Ref. 17. (a) FHNC, (b) STLS local-field corrections are used in conjunction with different screened inter-layer interaction models at  $T = 1\text{ K}$ . (c) Same as (a) at  $T = 4\text{ K}$ .

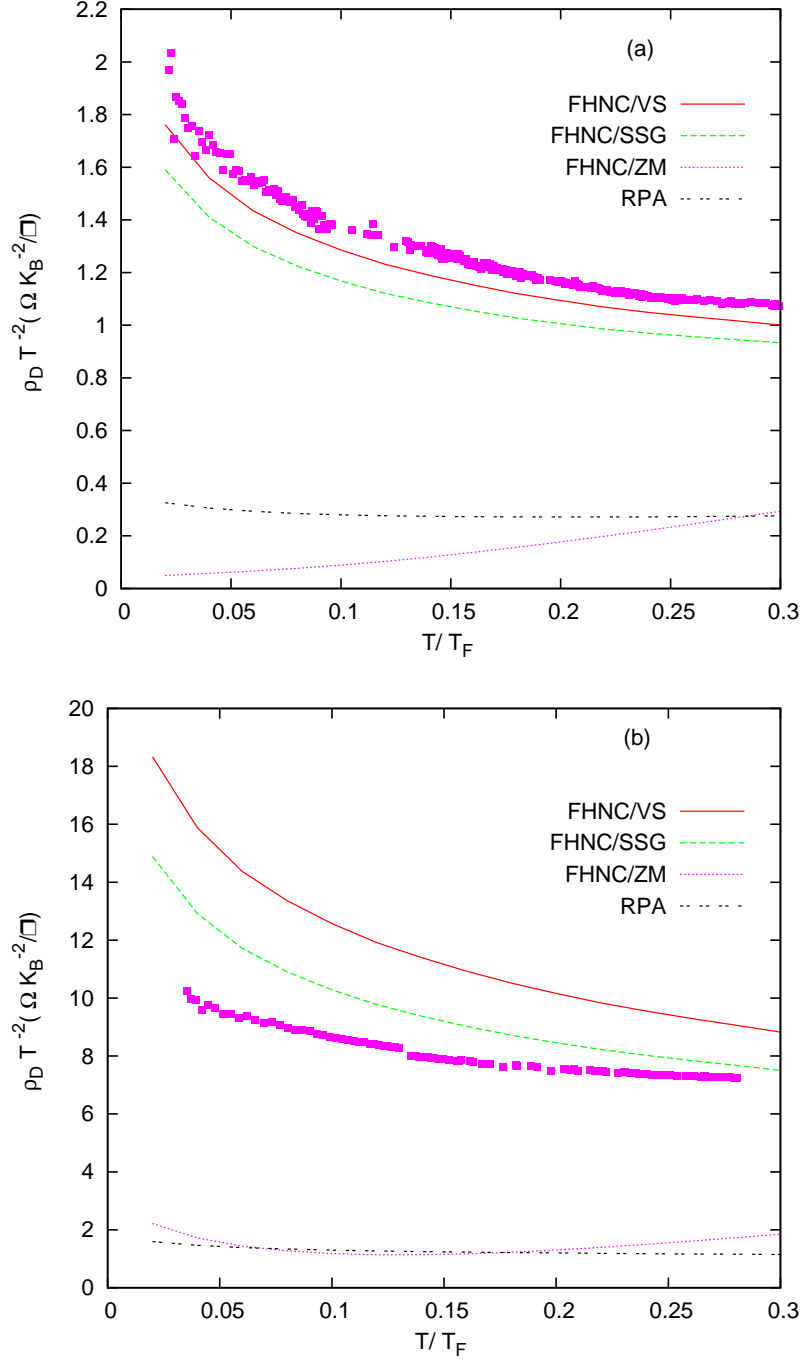


FIG. 6: (Color online) The scaled drag rate  $\rho_D/T^2$  as a function of temperature for (a)  $n = 3.8 \times 10^{10} \text{ cm}^{-2}$  ( $r_s = 2.93$ ) and (b)  $n = 2.3 \times 10^{10} \text{ cm}^{-2}$  ( $r_s = 3.77$ ). The full boxes are the experimental data of Ref. 8. FHNC local-field corrections used in conjunction with different inter-layer interaction models are compared with RPA.

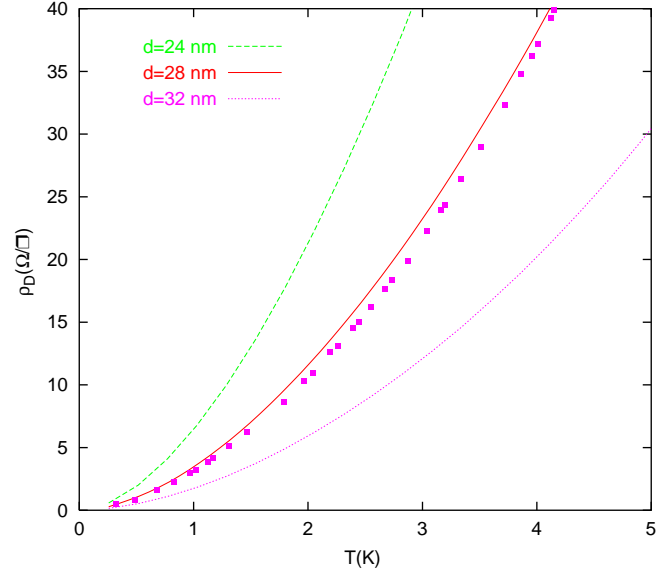


FIG. 7: (Color online) The temperature dependence of the drag resistivity for a bilayer electron system with layer density  $n = 3.1 \times 10^{10} \text{ cm}^{-2}$  ( $r_s = 3.25$ ). The full boxes are the experimental data of Ref. 8 at the same density and  $d = 280 \text{ \AA}$ .